2 PERKIN

Se–N interactions in selenohydroxylamine: a theoretical study

Prasad V. Bharatam,* Rajnish Moudgil and Damanjit Kaur

Department of Chemistry, Guru Nanak Dev University, Amritsar-143 005, India

Received (in Cambridge, UK) 29th June 2000, Accepted 15th September 2000
First published as an Advance Article on the web 9th November 2000

The potential energy surfaces of thiohydroxylamine HS–NH$_2$, **1**, and selenohydroxylamine HSe–NH$_2$, **2**, have been searched, using *ab initio* and density functional methods, to study the conformational preferences. There are two minima on the path of rotation around the Se–N bond in **2**. High accuracy G2MP2 calculations showed that the Se–N rotational barrier in **2** is 5.41 kcal mol^{-1}, which is 1.16 kcal mol^{-1} less than the S–N rotational barrier in **1**. The inversion around N in **1** and **2** goes through low energy barriers of 1.79 and 2.44 kcal mol^{-1} at the same level respectively. Charge analysis using the natural population analysis (NPA) method has been performed to understand the electronic factors responsible for the observed trends in the Se–N interactions. The strength of the negative hyperconjugation in **2** has been estimated using natural bond orbital (NBO) analysis and by studying the substituent effect.

Introduction

Organoselenium chemistry closely resembles the chemistry of organosulfur compounds.[1] The major differences between them arise from the larger size and polarizability of selenium relative to sulfur. Several selenols, selenones,[2] selenoamides,[3] selenonium ylides,[4] *etc.* have been synthesized and studied in comparison to the corresponding sulfur systems. Compounds with an Se–N bond are rare, though many compounds with S–N bonds like sulfonamides,[5] RO$_2$S–NR$_2$, sulfenamides,[6] RS–NR$_2$, sulfilimines,[7] R$_2$S=NR, sulfinimines,[8] R$_2$S–N=CH$_2$, *etc.* are well known. Flammang *et al.*[9a] have reported the generation of nitrile *N*-selenides in the gas phase, which have Se–N ionic interactions. They also reported the generation of pyridine *N*-selenide in the gas phase.[9b] Kamigata *et al.*[4,10] have reported the synthesis, kinetics, optical activity and Se–N interactions in selenonium imides, R$_2$Se=NR with Se–N ionic resonance interactions. Some cyclic systems like selenazines, selenodiazoles, Se$_4$N$_4$ *etc.* with an Se–N bond are known.[11] In contrast, very few studies have been reported on simple selenohydroxylamines (also known as selenamides and selenenamides) RSe–NR$_2$ with an Se–N single bond.[12] Selenamides are amides of selenenic acids and are in general prepared by the reaction of secondary amines with RSeCl, RSeBr, RSeOH *etc.* (R = phenyl). These can be used to prepare selenides, selenoacetates *etc.*[12a] Oxidation of selenamides RSe–NR$_2$ gives selenonamides RO$_2$Se–NR$_2$.[12e] Selenenylation of aldehydes is an important application of selenamides.[12h,i] The Se–N bond also adds across the C–C double bond in enones[12a] and the C–C triple bond in alkynes.[12j] The paucity of studies on the chemistry of selenamides is surprising because the corresponding sulfenamides[6] RS–NR$_2$ are well known; their chiroptical properties are well studied[13] and they are also reported to show very strong negative hyperconjugation.[14] In our laboratory we have been studying the bonding characteristics of selenoamides,[15] RCSeNH$_2$, selenonamides,[15] RO$_2$SeNH$_2$, isoselenocyanates, Se=C=NH, *etc.* to understand the bonding in organoselenium complexes and also studying the S–N interactions in organosulfur compounds.[16] In continuation of our efforts, we present studies on the conformational preferences of selenohydroxylamine, HSe–NH$_2$, **2**, (Fig. 1) using theoretical methods and compare them with those of thiohydroxylamine.

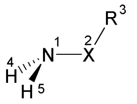

1 X = S, R = H
2 X = Se, R = H
3 X = Se, R = CH$_3$
4 X = Se, R = Cl
5 X = Se, R = F

Thiohydroxylamines are compounds with a variety of applications. These compounds possess only a single bond between sulfur and nitrogen, but show large rotation barriers, in the range 12–22 kcal mol^{-1}.[6] They show axial chirality and can be enantiomerically resolved.[13] The barrier to rotation of the S–N single bond has been argued to be mainly due to five factors. These are: (1) the four-electron interactions (lone pair–lone pair repulsions), (2) the two-electron interaction (negative hyperconjugation), (3) steric factors (arising from bulkiness of the substituent), (4) the electrosteric effects (arising from the substituents on the phenyl group attached to the sulfur atom), (5) the dπ–pπ interactions. Reed and Schleyer[14] showed that thiohydroxylamines show very strong negative hyperconjugation and dπ–pπ interactions are negligible. Following this, selenohydroxylamines are also expected to show strong negative hyperconjugation (also known as a generalized anomeric effect which represents the intramolecular donor–acceptor $n \rightarrow \sigma^*$ delocalizations leading to an in-plane π character) and large rotational barriers. We report G2MP2 estimates of rotational barriers in HS–NH$_2$, **1**, HSe–NH$_2$, **2**, and a study of substituent effects to understand the Se–N interactions in selenohydroxylamines. Natural bond orbital (NBO) analysis has been carried out to estimate the negative hyperconjugative interactions.

Computational details

Ab initio MO[17] and density functional (DFT)[18] calculations have been carried out using the GAUSSIAN94W[19] package, a Windows version of the GAUSSIAN94 suite of programs, on an IBM compatible PC Pentium-100 MHz with 64 MB memory and 1 GB disk space. Complete optimizations have been performed on thiohydroxylamine, **1**, and selenohydroxylamine, **2**, their rotational, N-inversion conformers and corresponding transition states using the MP2(Full)/6-31+G*[20] basis set. Since these molecules possess several lone pairs of electrons,

DOI: 10.1039/b005201i

Table 1 Various geometric parameters of thiohydroxylamine and selenohydroxylamine at the MP2(Full)/6-31+G* level. The bond lengths are in Å and angles are in degrees

	Thiohydroxylamine					Selenohydroxylamine			
	1	**1-r**	**1-rts**	**1-its**		**2**	**2-r**	**2-rts**	**2-its**
N1–S2	1.730	1.712	1.775	1.679	N1–Se2	1.862	1.846	1.907	1.804
N1–H4	1.016	1.016	1.021[b]	1.008	N1–H4	1.018	1.017	1.023[b]	1.008
N1–H5	1.016	1.016	1.021[b]	1.008	N1–H5	1.018	1.017	1.023[b]	1.008
S2–H3	1.341	1.352	1.340	1.351	Se2–H3	1.481	1.493	1.478	1.493
S2–N1–H4	110.7	113.7	106.2	120.7	Se2–N1–H4	109.3	111.7	107.0	120.6
S2–N1–H5	110.7	113.7	109.2	120.7	Se2–N1–H5	109.3	111.7	104.9	120.6
N1–S2–H3	96.5	102.2	96.4	100.9	N1–Se2–H3	95.00	101.5	95.50	99.60
H4–N1–S2–H3	119.3	64.0	224.4	90.4	H4–N1–Se2–H3	120.4	61.80	26.30	91.40
H4–N1–S2–H3	−119.3	−64.0	337.5	−90.4	H4–N1–Se2–H3	−120.4	−61.80	137.4	−91.40
φ[a]	330.6	338.0	320.5	360.0	φ[a]	327.6	333.4	316.9	359.9

[a] φ = sum of angles around nitrogen. [b] These values become exactly the same due to the rounding of the values up to the third decimal place. However, they are slightly different at higher decimal places giving only C_1 symmetry to **1-rts** and **2-rts**.

Table 2 Frequencies (cm^{-1}) of different normal modes of vibration in thiohydroxylamine and selenohydroxylamine along with IR intensities at the MP2(Full)/6-31+G* level

Thiohydroxylamine			Selenohydroxylamine		
Normal modes	Frequencies	Intensities	Normal modes	Frequencies	Intensities
Torsion	432.1	65.3	Torsion	379.3	51.9
S–N Stretching	660.4	96.2	Se–N Stretching	571.9	46.8
Scissoring	867.8	69.2	Scissoring	814.5	71.5
N–S–H Bending	1017.2	16.0	N–Se–H Bending	890.3	31.6
Twisting	1111.8	3.10	Twisting	1063.3	2.50
Wagging	1621.1	26.5	Wagging	1596.1	26.3
S–H Stretching	2624.8	19.0	Se–H Stretching	2335.8	26.9
N–H Stretching symmetric	3373.3	9.33	N–H Stretching symmetric	3355.7	14.5
N–H Stretching asymmetric	3477.5	35.3	N–H Stretching asymmetric	3464.7	35.9

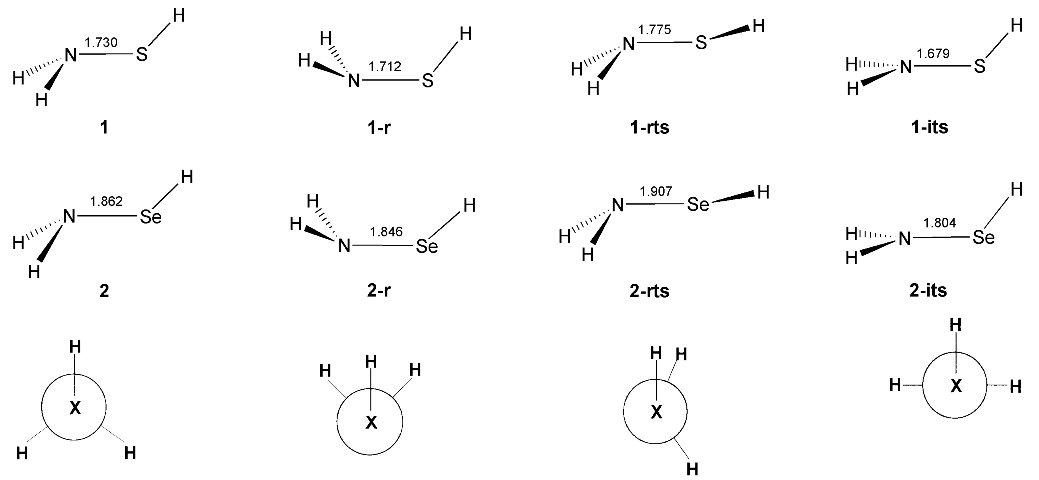

Fig. 1 Important structural features of thiohydroxylamine, **1** and selenohydroxylamine, **2** and their conformers (**-r**), rotational transition stares (**-rts**) and inversion transition states (**-its**). The given data are at the MP2 (Full)/6-31+G* level. Bond lengths are given in Å.

inclusion of diffuse functions in the basis set is important.[17] To study the effect of electron correlation on the geometries and energies, full optimizations have been performed using B3LYP/6-31+G*[21] levels. Frequencies were computed analytically for all optimized species at the MP2(Full)/6-31+G* level in order to characterize each stationary point as a minimum or a transition state and to determine the zero point vibrational energies (ZPE). The ZPE values have been scaled by a factor of 0.9153.[22] In order to obtain accurate values of the S–N and Se–N rotational barriers, calculations have been repeated at various levels of *ab initio* calculations including QCISD(T),[23] CCSD(T)[24] and G2MP2[25] methods as shown in Tables 1 and 2. Atomic charges in all the structures were obtained using the natural population analysis (NPA) method within the natural bond orbital approach[26] with the MP2 densities using the MP2(Full)/6-31+G* wavefunction. The substituent effect on the Se–N interaction has been studied using the MP2/6-31+G* level on XSe–NH$_2$ (X = Me, Cl, F). MP2(Full)/6-31+G* geometric parameters and G2MP2 energies will be used in the discussion unless otherwise specifically mentioned.

Results and discussion

On the potential energy surface of selenohydroxylamine, HSe–NH$_2$, two minima, **2**, **2-r**, one rotational transition state, **2-rts**, and one inversion transition state, **2-its**, could be located as

Table 3 Absolute energies (in a.u.) and zero point energies (ZPE, in kcal mol^{-1}) obtained at various levels for **1** and **2** and their different conformers

Thiohydroxylamine				
Method	**1**	**1-r**	**1-rts**	**1-its**
B3LYP/6-31+G*	−454.723402	−454.722041	−454.710317	−454.719264
MP2(Full)/6-31+G*	−453.983706	−453.982175	−453.969890	−453.979096
QCISD(T)/6-31+G*//MP2(Full)/6-31+G*	−454.004949	−454.003278	−453.992024	−453.999319
CCSD(T)/6-31+G*//MP2(Full)/6-31+G*	−454.004773	−454.003102	−453.991848	−453.999150
G2MP2	−454.171981	−454.171762	−454.161509	−454.169132
ZPE[a] (NIF)	22.11(0)	22.03(0)	21.53(1)	21.26(1)
Selenohydroxylamine				
Method	**2**	**2-r**	**2-rts**	**2-its**
B3LYP/6-31+G*	−2455.929739	−2455.929591	−2455.919147	−2455.925149
MP2(Full)/6-31+G*	−2454.079568	−2454.079070	−2454.068153	−2454.074332
QCISD(T)/6-31+G*//MP2(Full)/6-31+G*	−2454.075790	−2454.075189	−2454.065208	−2454.069486
CCSD(T)/6-31+G*//MP2(Full)/6-31+G*	−2454.075769	−2454.074982	−2454.065004	−2454.069288
G2MP2	−2456.418673	−2456.418553	−2456.410047	−2456.414779
ZPE[a] (NIF)	23.04(0)	22.04(0)	22.52(1)	22.10(1)

[a] Obtained at the HF/6-31+G* level and scaled by 0.9153; NIF: number of imaginary frequencies.

Table 4 Energy difference between the two ground state conformers (Δ*E*), X–N rotational barriers, and N-inversion barriers of thiohydroxylamine and selenohydroxylamine. All the values are ZPE corrected and are in kcal mol^{-1}

	Thiohydroxylamine			Selenohydroxylamine		
Method	Δ*E*	Rotation barriers	Inversion barriers	Δ*E*	Rotation barriers	Inversion barriers
B3LYP/6-31+G*	0.77	7.63	1.74	0.03	6.12	1.93
MP2(Full)/6-31+G*	0.88	8.09	2.04	0.25	6.64	2.34
QCISD(T)/6-31+G*	0.94	7.53	2.68	0.32	6.12	3.95
CCSD(T)/6-31+G*	0.97	7.53	2.68	0.43	6.11	4.06
G2MP2	0.14	6.57	1.79	0.07	5.41	2.44

in the case of sulfenamide (**1**, **1-r**, **1-rts**, **1-its**). The structural data corresponding to these structures obtained using the MP2(Full)/6-31+G* level are given in Table 1. Both the ground state structures **2** and **2-r** are found to have C_s symmetry. The basic difference between the two structures arises from the arrangement of the NH_2 group *syn* (**2-r**) or *anti* (**2**) with respect to the Se–H bond. The Se–N bond length in **2** is 1.862 Å at the MP2(Full)/6-31+G* level, slightly less than the sum of covalent radii (1.88 Å) of Se and N.[27] This may be due to anomeric π character as in **1**. The calculated Se–N distance is comparable to the Se–N distance in 4-[(2-nitrophenyl)selenyl]-morpholine (1.869 Å) and is longer than the Se–N distance in $C_6H_5O_2Se–NMe_2$ 1.815 Å.[12e] The calculated Se–N distances at the HF/6-31+G*, MP2(Full)/6-31+G* and B3LYP/6-31+G* levels are 1.833, 1.862 and 1.873 Å respectively. The value obtained at the MP2(Full)/6-31+G* level matches well the experimental value (1.869 Å). The N–Se–H angle in **2** is 95.0°, only slightly larger than the H–Se–H angle (91°) in SeH_2,[27b] and comparable to the small N–S–H angle (96.5°) in **1**. The pyramidalization at nitrogen in **2** is more than that in **1** as indicated by sum of the angles around nitrogen, 327.6 and 330.6° respectively. This indicates that lone pair electrons on nitrogen are more localized in **2** in comparison to **1**. The calculated frequencies of **2** along with estimated intensities are given in Table 2. The Se–N stretching frequencies are in the range 570–590 cm^{-1} and show strong mixing with the frequencies corresponding to NH_2 scissoring and N–Se–H bending motions. The Se–H stretching frequencies are in the range 2340–2350 cm^{-1}. The calculated frequencies of **1** and **2** can be easily correlated.

In **2-r** also the N atom has a pyramidal arrangement but to a lesser degree (the sum of the angles around nitrogen is 333.4°). The Se–N bond length in **2-r** is smaller than that in **2**. The Se–N–H and N–Se–H angles are larger in **2** as compared to those in **1**. All these observations indicate stronger negative hyperconjugation in **2-r** relative to **2**. The differences in the geometric parameters of **2** and **2-r** are similar to those observed between **1** and **1-r**. In the rotational transition state **2-rts**, the Se–N bond length is elongated by ~0.45 Å. This elongation is mainly due to the loss of anomeric π character. In **2-rts**, the pyramidal character has increased as expected, the sum of the angles around nitrogen is 316.9°. The inversion transition state **2-its** also has C_s symmetry with an sp^2 arrangement around nitrogen. The Se–N bond in **2-its** is shorter by ~0.06 Å. These variations in the geometric parameters during rotation and inversion can be attributed to the variation in the $n_{(N)}\rightarrow\sigma^*_{SeH}$ negative hyperconjugation. The observed variation in **2** is relatively smaller than that in **1** and hence it can be inferred that the negative hyperconjugation is relatively weak in **2** in comparison to that in **1**.

The absolute energies and the ZPE values of **1**, **2** and related structures are given in Table 3, the relative values are given in Table 4. The energy difference (Δ*E*) between the rotamers in **1** is 0.14 kcal mol^{-1} and in **2** Δ*E* is 0.07 kcal mol^{-1} at the G2MP2 level. The calculated inversion barriers in **1** and **2** are 1.79 and 2.44 kcal mol^{-1} at the G2MP2 level. These values are much smaller than the inversion barriers in NH_3 (4.20 kcal mol^{-1} at the G2MP2 level), indicating virtual indistinguishability of the conformers at room temperature. The smaller N-inversion barriers can be attributed to the presence of $n_{(N)}\rightarrow\sigma^*_{X–H}$ negative hyperconjugation, which stabilizes the inversion transition structures **1-its** and **2-its**. The stronger negative hyperconjugation in **2-its** is evidenced by the decrease in Se–N distance, increase in Se–N bond polarization (Table 5) and increase in the N–Se–H and Se–N–H angles in **2-its** in com-

Table 5 Parameters from NBO analysis contributing to the second-order estimate $E^{(2)}$ of $n_{(N)}\rightarrow\sigma^*_{X-H}$ interaction strength at the MP2(Full)/6-31+G* level

	q^a										
	N	S	H	H	H	3d[b]	$\rho(n)$[c]	$\rho(\sigma^*)$[d]	$E^{(2)}$[e]	$\varepsilon_j - \varepsilon_i$[f]	F_{ij}[g]
1	−1.089	0.147	0.119	0.412	0.412	0.03	1.938	0.014	4.60	0.97	0.060
1-r	−1.095	0.192	0.083	0.410	0.410	0.03	1.973	0.023	8.09	0.93	0.078
1-rts	−1.054	0.140	0.109	0.400	0.405	0.03	1.995	0.005	—	—	—
1-its	−1.161	0.215	0.090	0.428	0.428	0.03	1.966	0.026	10.3	0.86	0.084
	N	Se	H	H	H	4d[b]					
2	−1.136	0.255	0.056	0.412	0.412	0.03	1.984	0.015	4.74	0.87	0.057
2-r	−1.141	0.298	0.019	0.412	0.412	0.03	1.975	0.023	7.08	0.85	0.069
2-rts	−1.097	0.244	0.047	0.402	0.404	0.03	1.996	0.005	—	—	—
2-its	−1.224	0.338	0.025	0.431	0.431	0.03	1.967	0.028	10.1	0.75	0.078

[a] Atomic charges obtained using the NPA method. [b] Occupation of d-orbitals. [c] Occupancy of the nitrogen lone pair. [d] Occupancy of the X–H σ* MO. [e] The energy corresponding to $n_{(N)}\rightarrow\sigma^*_{X-H}$ delocalization. [f] Energy difference between $n_{(N)}$ and σ^*_{X-H} molecular orbitals. [g] Fock matrix element corresponding to $n_{(N)}\rightarrow\sigma^*_{X-H}$ overlap.

parison to those in **2**. The relatively higher inversion barrier in **2** supports the observation that negative hyperconjugation is smaller in selenohydroxylamine **2** in comparison to that in **1**.

The Se–N rotational barrier in **2** at the MP2(Full)/6-31+G* level is 6.64 kcal mol^{-1}. Inclusion of electron correlation using the density functional B3LYP method gives a Se–N rotational barrier of 6.12 kcal mol^{-1}. When electron correlation is employed using the QCISD(T) and CCSD(T) levels, the rotational barrier becomes 6.12 and 6.11 kcal mol^{-1} respectively, comparable to the values obtained using the B3LYP/6-31+G* level. However, at the high accuracy G2MP2 level, the rotational barrier gets reduced to 5.41 kcal mol^{-1}. The Se–N rotational barrier is about 2.8 kcal mol^{-1} higher than the C–C single bond rotation in ethane (2.6 kcal mol^{-1} at the G2MP2 level). The Se–N rotational barrier in **2** (5.41 kcal mol^{-1}) is less than the S–N rotational barrier (6.57 kcal mol^{-1}) in **1** at the G2MP2 level. The high rotational barriers in thiohydroxylamines have been attributed mainly to the negative hyperconjugation ($n_{(N)}\rightarrow\sigma^*_{S-H}$).[14] The reduced Se–N rotational barrier might be due to smaller negative hyperconjugation in **2**, which may arise from the longer bond length (Se–N: 1.862 Å in **2** and S–N: 1.730 Å in **1**, both at the MP2(Full)/6-31+G* level).

NBO analysis

Atomic charges obtained by using the NPA method are given in Table 5. The data clearly indicate that the N atom has a unit negative charge whereas the selenium is only slightly positive. In **2-r**, the negative charge on nitrogen slightly increases and the positive charge on selenium increases by 0.043 units, *i.e.* the Se–N bond polarization increases. This increase in polarization is due to the increases in the N–Se–H and Se–N–H angles which increase the s character at N and Se atoms. Because of this increase in the polarization, the electrostatic attraction between selenium and nitrogen increases which finally leads to a decrease in the Se–N distance, in accordance with the negative hyperconjugation present in these systems. In the inversion transition state **2-its**, the s character and electronegativity of N are more than those in **2**, resulting in the increase in the charge at N and reduction in the Se–N bond. This analysis indicates that the smaller Se–N bond distances in **1-its** and **2-its** with an almost planar arrangement on nitrogen are due more to increased charge separation (as a consequence of increased negative hyperconjugation) between Se and N than to the increase in the charge transfer from N to Se through d-orbital interactions. The group charges in **1** and **2** indicate that the Se–N bond is more polarized than the S–N bond. This is consistent with the expected increase in the ionic character of the X–N bond as we move down a group. The Se–N bond in **2** has stronger ionic character than the S–N bond in **1**. Experimentally, RSe–NR$_2$ behaves like HBr and adds across double bonds,[12a] whereas no reports of such behaviour are available for RS–NR$_2$. This may be justified in terms of the stronger ionic character of Se–N bonds.

NBO analysis (Table 5) shows that the occupancy of the nitrogen lone pair is only 1.984 in **2**. The occupancy of the σ^*_{Se-H} orbital is 0.015. This clearly suggests that $n_{(N)}\rightarrow\sigma^*_{Se-H}$ charge transfer is taking place in **2**. The second-order energy analysis[26] shows that the energy associated with this transfer is 4.74 kcal mol^{-1} (this is the largest second order interaction found in **2**, the second largest (2.99 kcal mol^{-1}) corresponding to $\sigma_{Se-H}\rightarrow$N Rydberg orbital). The energy difference between the $n_{(N)}$ and σ^*_{Se-H} orbitals is 0.87 au and the Fock matrix element representing this overlap has a value of 0.057 au. Comparison of these values of **1** and **2** suggests that the strength of negative hyperconjugation in these two systems is almost equal. The $\Delta\varepsilon_{ij}$ between the interacting MOs is smaller in **2** compared to that in **1**, which should have increased the negative hyperconjugative interactions, because this value appears in the denominator.[26] However, the overlap between the two orbitals is also decreasing as indicated by the decrease in Fock matrix element values. Hence the decrease in the Se–N rotation barrier in selenohydroxylamines is mainly due to the decrease in the overlap between the $n_{(N)}$ and σ^*_{Se-H}.[28] This can be traced to the longer bond length in Se–N relative to S–N, which in turn originates from the larger size of Se.

Substituent effect

Negative hyperconjugation gets strongly enhanced when hydrogen is replaced by electronegative elements like fluorine and chlorine. To estimate the increase in the negative hyperconjugation across the Se–N bond, MP2/6-31+G* level calculations have been performed on CH$_3$Se–NH$_2$, **3**, ClSe–NH$_2$, **4**, and FSe–NH$_2$, **5**. Table 6 gives a comparison between geometric parameters, Se–N rotational barriers, and energy of stabilization due to substitution. The Se–N distance decreases with an increase in the electronegativity of the substituent. The calculated bond lengths at the MP2/6-31+G* level are 1.872 > 1.867 > 1.792 > 1.772 Å for X = CH$_3$, H, Cl, F respectively. The Se–N bond rotational barrier (6.56 kcal mol^{-1}) in **2** becomes doubled (13.72 kcal mol^{-1}) with chlorine substitution and further increases to 16.46 kcal mol^{-1} with fluorine substitution. Both **4** and **5** have only one conformer, with a *syn* arrangement. Rotamers **4-r** and **5-r** could not be located on the respective PE surfaces, and hence inversion barriers cannot be calculated. The calculated rotational barriers for **2**–**5** are consistently less than the rotational barriers in the corresponding thiohydroxylamine

Table 6 Important parameters corresponding to substituent effects in **1** and **2** at the MP2/6-31+G* level

	Thiohydroxylamine, $RSNH_2$					Selenohydroxylamine, $RSeNH_2$			
	R = H	CH_3	Cl	F		R = H	CH_3	Cl	F
S–N[a]	1.732	1.730	1.647	1.629	Se–N[a]	1.867	1.872	1.792	1.772
S–N–H[b]	110.6	111.1	117.8	119.1	Se–N–H[b]	109.2	109.6	115.7	117.5
N–S–X[b]	96.5	98.5	106.8	104.7	N–Se–X[b]	95.0	95.7	105.4	103.8
S–N rotational barriers[c]	8.04	8.17	16.18	20.20	Se–N rotational barriers[c]	6.56	6.84	13.72	16.46
N-inversion barriers[c]	2.04	—	—	—	N-inversion barriers[c]	2.47	—	—	—
ΔE[c]	—	—	14.77	21.02	ΔE[c]	—	—	11.93	14.46
Atomic charge on					Atomic charge on				
S	0.114	0.346	0.451	0.745	Se	0.206	0.428	0.562	0.850
N	−1.072	−1.078	−1.056	−1.078	N	−1.109	−1.115	−1.119	−1.148

[a] Bond lengths in Å. [b] Angles in degrees. [c] Energies in kcal mol^{-1}. ΔE = stabilization due to substitution.

systems. This indicates that selenohydroxylamines with substituents which enhance negative hyperconjugation may show axial chirality similar to thiohydroxylamine. However, the enantiomer separation[13] might prove relatively more difficult. Stabilization due to substitution can be calculated using isodesmic equations (for example, eqn. (1)). The additional

$$FX\text{–}NH_2 + XH_2 \longrightarrow HX\text{–}NH_2 + FXH \qquad (1)$$

stabilization gained by selenohydroxylamine is 11.93 and 14.46 kcal mol^{-1} due to chlorine and fluorine substitution respectively at the MP2/6-31+G* level. These high stabilization values indicate that there is a strong increase in the negative hyperconjugation upon substitution though it is less pronounced than that in thiohydroxylamine. This also supports an earlier observation that selenohydroxylamine has relatively weaker negative hyperconjugation.

Conclusions

Theoretical studies show that selenohydroxylamines closely resemble thiohydroxylamine. They show strong negative hyperconjugation, though relatively less than thiohydroxylamine. The rotational barriers in selenohydroxylamine are only slightly less than those of thiohydroxylamine and hence selenohydroxylamines may also show axial chirality. The NBO analysis shows that the weaker negative hyperconjugation in selenohydroxylamines can be traced to the reduced overlap between $n_{(N)}$ and $\sigma^*_{Se\text{–}H}$ MOs. It can be finally concluded that the Se–N interactions are characterized by a regular covalent bond, and an additional in-plane π bond due to negative hyperconjugation. The ionic character across the Se–N bond in **2** is stronger than the ionic character across the S–N bond in **1**.

Acknowledgements

The authors thank the Department of Science and Technology (DST), New Delhi for financial support.

References

1 (*a*) G. H. Whitham, *Organosulphur chemistry*, Oxford University Press, New York, 1995, p. 85; (*b*) A. Krief, in *Comprehensive Organic Synthesis*, ed. B. M. Trost, Pergamon Press, Oxford, 1993, vol. 1, pp. 629–728; (*c*) D. Liotta, *Organoselenium Chemistry*, Wiley-Interscience, New York, 1987.

2 N. Kamigata and T. Shimizu, *Rev. Heteroat. Chem.*, 1991, **4**, 226.

3 (*a*) M. D. Ruan, P. F. Zhang, Y. Tao and W. Q. Fan, *Synth. Commun.*, 1996, **26**, 2617; (*b*) M. Segi, T. Takahashi, I. H. Ichinose, G. M. Li and T. Nakajima, *Tetrahedron Lett.*, 1992, **33**, 7865.

4 N. Kamigata, Y. Nakamura, K. Kikuchi, I. Ikemoto, T. Shimizu and H. Matsuyama, *J. Chem. Soc.*, *Perkin Trans. 1*, 1992, 1721.

5 P. G. Sammes, in *Comprehensive Medicinal Chemistry*, ed. C. Hansch, Pergamon Press, London, 1990, vol. 2, p. 255.

6 (*a*) L. Craine and M. Raban, *Chem. Rev.*, 1989, **89**, 689; (*b*) M. D. Refvik and A. L. Schwan, *J. Org. Chem.*, 1996, **61**, 4232; (*c*) G. Celentano, S. Colonna, N. Gaggero and C. Richelmi, *Chem. Commun.*, 1998, 701; (*d*) A. Bagno, S. J. Eustace, L. Johansson and G. Scorrano, *J. Org. Chem.*, 1994, **59**, 232; (*e*) E. L. Clennan and H. Zhang, *J. Am. Chem. Soc.*, 1994, **116**, 809; (*f*) V. Clarke and E. R. Cole, *Phosphorus, Sulfur Silicon Relat. Elem.*, 1994, **92**, 45; (*g*) G. Capozzi, L. Gori, S. Menichetti and C. Nativi, *J. Chem. Soc.*, *Perkin Trans. 1*, 1992, 1923.

7 T. L. Gilchrist and C. J. Moody, *Chem. Rev.*, 1977, **77**, 409.

8 (*a*) F. A. Davis, R. E. Reddy, J. M. Szewezyk, G. V. Reddy, P. S. Portonova, H. Zhang, D. Fanelli, R. T. Reddy, P. Zhou and P. J. Carrol, *J. Org. Chem.*, 1997, **62**, 2555; (*b*) F. A. Davis, P. Zhou and B. C. Chen, *Chem. Soc. Rev.*, 1998, **27**, 13.

9 (*a*) P. Gerbaux, R. Flammang, E. H. Morkved, M. W. Wong and C. Wentrup, *Tetrahedron*, 1998, **39**, 533; (*b*) R. Flammang, *Int. J. Mass Spectrom. Ion Processes*, 1999, **184**, 39; (*c*) C. L. Pederson, N. Harrit, M. Poliakoff and I. Dunkin, *Acta Chem. Scand., Ser. B*, 1997, **31**, 848; (*d*) C. L. Pederson and N. Hacker, *Tetrahedron Lett.*, 1997, **45**, 3981.

10 (*a*) T. Shimizu, N. Kamigata and S. Ikuta *J. Chem. Soc.*, *Perkin Trans. 2*, 1999, 1469; (*b*) T. Shimizu, N. Seki, H. Taka and N. Kamigata, *J. Org. Chem.*, 1996, **61**, 6013; (*c*) N. Kamigata, H. Taka, A. Matsuhisa, H. Matsuyama and T. Shimizu, *J. Chem. Soc.*, *Perkin Trans. 1*, 1994, 2257; (*d*) N. Kamigata, H. Taka, A. Matusuhisa and T. Shimizu, *J. Phys. Org. Chem.*, 1995, **8**, 139.

11 (*a*) M. Sainsbury, (Neth) *Rodd's Chem. Carbon Compounds*, 2nd edn., Elsevier, Amsterdam, 1998, vol. 4, p. 609; (*b*) A. P. Bradley and J. D. Wilkins, *Prog. Heterocycl. Chem.*, 1998, **10**, 172; (*c*) J. S. Kwiatkowski and J. Leszczvnski, *J. Mol. Struct.*, 1997, **436–437**, 451.

12 (*a*) H. J. Reich and J. M. Renga, *J. Org. Chem.*, 1975, **40**, 3313; (*b*) T. G. Beck and R. G. Kerr, *Can. J. Chem.*, 1986, **64**, 308; (*c*) T. Shuji, T. Yoshito and N. Yujiro, *Synthesis*, 1995, **2**, 212; (*d*) C. Gicquel-Mayer, G. Perez, P. Lerouge and C. Paulmier, *Acta Crystallogr.*, *Sect. C*, 1987, **43**, 284; (*e*) Z. Zak, J. Merek and L. Kaznikl, *Z. Anorg. Allg. Chem.*, 1996, **622**, 1101; (*f*) P. Ruostesuo, A. M. Hakkinen, R. Liias-Lepisto and U. Salminer, *Spectrochim. Acta*, *Part A*, 1988, **44**, 1105; (*g*) C. Paulmier, P. Lerouge, F. Outurquin, S. Chapella and P. Granger, *Magn. Reson. Chem.*, 1987, **25**, 955; (*h*) M. Jefson and J. Meinwald, *Tetrahedron Lett.*, 1981, **22**, 3561; (*i*) C. Paulmier and P. Lerouge, *Tetrahedron Lett.*, 1982, **23**, 1557; (*j*) A. Krief, in *Comprehensive Organic Synthesis*, ed. B. M. Trost, Pergamon Press, Oxford, 1993, vol. 1, p. 658; (*k*) X. Wang, K. N. Houk, M. Spichty and T. Wirth, *J. Am. Chem. Soc.*, 1999, **121**, 8567; (*l*) H. J. Reich, J. M. Renga and J. E. Trend, *Tetrahedron Lett.*, 1976, **26**, 2217; (*m*) K. M. Sun, R. M. Giuliano and B. F. Reid, *J. Org. Chem.*, 1985, **50**, 4774; (*n*) M. E. Kuchne and P. J. Seator, *J. Org. Chem.*, 1985, **50**, 4790.

13 M. B. D. Blanca, E. Maimon and D. Kost, *Angew. Chem.*, *Int. Ed. Engl.*, 1997, **36**, 2216.

14 A. E. Reed and P. v. R. Schleyer, *Inorg. Chem.*, 1998, **27**, 3969.

15 P. V. Bharatam, P. Uppal and P. S. Bassi, *J. Chem. Phys.*, 1997, **276**, 31.

16 (*a*) P. V. Bharatam, P. Uppal, Amita and D. Kaur, *J. Chem. Soc.*, *Perkin Trans. 2*, 2000, 43; (*b*) P. V. Bharatam, Amita, P. Uppal and D. Kaur, *Indian J. Chem.*, *Sect. B*, 2000, **39**, in the press.

17 (*a*) W. J. Hehre, L. Radom, P. v. R. Schleyer and J. A. Pople, *Ab Initio Molecular Orbital Theory*, Wiley-Interscience, New York, 1986; (*b*) J. B. Foresman and E. Frisch, *Exploring Chemistry with Electronic Structure Methods*, 2nd edn., Gaussian Inc., Pittsburgh, 1996.

18 (*a*) R. G. Parr and W. Yang, *Density-Functional Theory of Atoms and Molecules*, Oxford University Press, New York, 1989; (*b*) L. J. Bartolotti and K. Fluchick, in *Reviews in Computational Chemistry*, vol. 7, eds. K. B. Lipkowitz and D. B. Boyd, VCH Publishers, New York, 1996, pp. 187–216.

19 GAUSSIAN94, Revision B.2, M. J. Frisch, C. W. Trucks, H. B. Schlegel, P. M. W. Gill, B. G. Johnson, M. A. Robb, J. R. Cheeseman, T. Keith, G. A. Petersson, J. A. Montgomery, K. Raghavachari, M. A. Al-Laham, V. G. Zakrzewski, J. V. Ortiz, J. B. Foresman, C. Y. Peng, P. Y. Ayala, W. Chen, M. W. Wong, J. L. Andres, E. S. Replogle, R. Gomperts, R. L. Martin, D. J. Fox, J. S. Binkley, D. J. Defrees, J. Baker, J. J. P. Stewart, M. Head-Gordon, C. Gonzalez and J. A. Pople, Gaussian, Inc., Pittsburgh, PA, 1995.

20 R. Krishnan, M. J. Frisch and J. A. Pople, *J. Chem. Phys.*, 1980, **72**, 4244.

21 (*a*) A. D. Becke, *J. Chem. Phys.*, 1993, **98**, 5648; (*b*) C. Lee, W. Yang and R. G. Parr, *Phys. Rev. B*, 1980, **37**, 785; (*c*) J. P. Perdew and Y. Wang, *Phys. Rev. B*, 1992, **45**, 13244.

22 A. P. Scott and L. Radom, *J. Phys. Chem.*, 1996, **100**, 16502.

23 J. A. Pople, M. Head-Gordon and K. Raghavachari, *J. Chem. Phys.*, 1987, **87**, 5968.

24 G. D. Purvis and R. J. Bartlett, *J. Chem. Phys.*, 1982, **76**, 1910.

25 L. A. Curtiss, K. Raghavachari and J. A. Pople, *J. Chem. Phys.*, 1993, **98**, 1293.

26 (*a*) A. E. Reed, R. B. Weinstock and F. Weinhold, *J. Chem. Phys.*, 1985, **83**, 735; (*b*) A. E. Reed, L. A. Curtiss and F. Weinhold, *Chem. Rev.*, 1988, **88**, 899.

27 (*a*) J. D. Lee, *Concise Inorganic Chemistry*, 4th edn., ELBS, London, 1994, p. 147; (*b*) J. D. Lee, *Concise Inorganic Chemistry*, 4th edn., ELBS, London, 1994, p. 568.

28 U. Salzner and P. v. R. Schleyer, *J. Am. Chem. Soc.*, 1993, **115**, 10231.